Available online at www.sciencedirect.com
SCIENCE DIRECT®
Scripta Materialia 51 (2004) 37–41
Scripta MATERIALIA
www.actamat-journals.com

Static and dynamic mechanical damage mechanisms in TiC-1080 steel cermets

W.D. Kaplan [a,*], D. Rittel [b], M. Lieberthal [a], N. Frage [c], M.P. Dariel [c]

[a] Department of Materials Engineering, Technion—Israel Institute of Technology, Haifa 32000, Israel
[b] Department of Mechanical Engineering, Technion—Israel Institute of Technology, Haifa 32000, Israel
[c] Department of Materials Engineering, Ben-Gurion University, Beer-Sheva 84105, Israel

Received 11 January 2004; received in revised form 11 March 2004; accepted 18 March 2004
Available online 17 April 2004

Abstract

Mechanical damage mechanisms in TiC-1080 steel cermets were characterized by transmission electron microscopy. Quasi-static failure occurs by blunting of interfacial flaws, and by interfacial cracking, with subsequent propagation into the steel matrix. Dynamic loading induces an additional failure mechanism of transgranular TiC cracking without extension to the steel matrix.

Keywords: Dynamic mechanical analysis; TEM; Interfaces; Composites

1. Introduction

TiC-1080 steel cermets have been prepared by liquid metal infiltration of a porous TiC matrix (30% open porosity) [1]. Various heat treatments were applied (as-received, quenched, tempered at 200, 300, and 400 °C). The dynamic strength and fracture properties of TiC-1080 steel cermets have been recently reported [2]. One key result was that the dynamic apparent K_{Id} was found to be on the average 3 times higher than its quasi-static counterpart. All the specimens exhibited essentially identical failure mechanisms, i.e. cleavage of the TiC network and steel matrix, irrespective of the loading rate and heat treatment. However, longitudinal cross-sections across the main fracture plane revealed a large number of arrested micro-cracks in the TiC phase of the dynamically fractured specimens only. It was suggested that additional energy is used in creating the secondary micro-cracks, thus raising the dynamic initiation toughness of the material. The present study reports a detailed TEM study of the damage mechanisms of TiC-1080 steel cermets.

2. Experimental methods

2.1. Processing

The selected cermet is a TiC-carbon steel composite. Although the dynamic properties of dense TiC ceramics are not high, they present some definite advantages. Ceramic TiC matrices with controlled open porosity (preforms) can be manufactured easily. Moreover, owing to the good wetting of TiC by molten steel, the porous preforms can be completely infiltrated by the molten metal. By varying the heat treatment applied to the cermet, the state of the metallic component can be changed while that of the ceramic matrix is kept constant. The TiC-steel cermets in this study consisted of two interpenetrating and interconnected, ceramic and metal, networks. They were fabricated by infiltrating porous TiC preforms with molten 1080 carbon steel. Titanium carbide, (CERAC®, Cat. No. T-1151, 325 mesh) powder was compressed at 35 MPa and sintered at 1600 °C for 60 min in a graphite furnace. At the outcome of this treatment, and as long as the same initial powder was used, reproducible preforms were obtained with roughly 30% total porosity. Infiltration by molten steel was conducted under vacuum at 10^{-4} Torr and 1500 °C for 30 min, followed by furnace cooling. The thermal treatments of the infiltrated TiC-steel

* Corresponding author. Tel./fax: +972-48294580.
E-mail address: kaplan@tx.technion.ac.il (W.D. Kaplan).

1359-6462/$ - see front matter
doi:10.1016/j.scriptamat.2004.03.021

cermets consisted of austenitization in evacuated quartz capsules, for 1 h at 870 °C, followed by furnace cooling or immersing and shattering the capsules in water. Tempering was conducted in air at 200, 300, or 400 °C for 1 hour.

2.2. Mechanical testing

The quasi-static apparent fracture toughness (K_{Ic}) was measured by three-point bending of notched bars, on a MTS 810 servo-hydraulic testing machine, under displacement control. Typical specimen dimensions were 20–40 mm in length, 4–5 mm in thickness and 4.5–5.5 mm in height. Since fatigue precracking is a delicate task, 2–3 mm long notches were machined with a 0.2 mm root radius diamond blade. Consequently, the reported (apparent) fracture toughness values, both static and dynamic, most likely overestimate the true fracture toughness that would be obtained from a fatigue precrack. The crosshead velocity was fixed to 0.083 mm/s. A two-dimensional finite element model (plane-strain) was run on ANSYS (1994) finite element code. For each specimen tested, the stress intensity factor corresponding to a unit load was calculated. The (apparent) fracture toughness was thus determined by multiplying the unit stress intensity factor by the maximum (fracture) load.

The apparent dynamic fracture toughness (K_{Id}) was determined from one-point impact bend tests. The procedure has been described in detail, and its validity has been assessed [3]. For the sake of brevity, we will only outline the main characteristics of the procedure. The main idea is that, based on the linearity of the fracture process (LEFM assumptions), the evolution of the stress intensity factor(s) can be determined if the loading force is known, and if the response of the structure to unit impulse is determined. In other words, if the applied load $F(t)$ is determined from a one-point impact test, and if $k_\delta(t)$ is the stress intensity resulting from a unit impulse, then the evolution of the stress intensity factor is given by:

$$K(t) = F(t) \ * \ k_\delta(t) \tag{1}$$

where the $*$ sign indicates a time convolution integral. Therefore, if the fracture time (t_{frac}) is determined, the fracture toughness is the value of the stress intensity factor at fracture.

The specimens were loaded by means of an instrumented Hopkinson bar, and fracture time was detected using single wire fracture gauges. The reader is referred to [3] for additional details on the experimental procedure. The typical valid sample size was at least 15 specimens per grade, on the average.

2.3. Characterization

Specimens for transmission electron microscopy (TEM) investigations were cut from bulk specimens or from an area immediately adjacent and parallel to the fracture surface of mechanically tested specimens. Specimens were cut using a diamond wafer blade, and mechanically thinned to ~100 μm by polishing with 15 μm grit diamond paste on the side *opposite* to the fracture surface. This was followed by mechanical dimpling, again on the side opposite to the fracture surface, and ion milling (5.0 kV argon) to perforation. TEM was conducted at 200 kV (JEOL 2000FX).

3. Results and discussion

3.1. Mechanical properties

Tables 1 and 2 summarize the apparent fracture toughness (quasi-static and dynamic) of the investigated cermets. The results clearly show that the dynamic initiation toughness is significantly higher than its static counterpart, regardless of the thermal treatment applied. For this material, the representative measured yield (fracture) strength of about 2000 MPa validates the specimen dimensions versus the apparent measured fracture toughness.

3.2. General microstructure

The general microstructure is composed of a matrix of TiC grains, with a maximum TiC grain size of ~30 μm. The infiltration of 1040 steel was almost complete, and very few residual pores were found. Penetration of the liquid metal reached geometrically complex regions, such as shown in Fig. 1, indicating a contact angle well below 90° (good liquid–solid wetting) in this system [4].

Table 1
Summary of results for the quasi static fracture apparent toughness K_{Ic}

Group	K_{Ic} average + 90% CI (MPa m$^{1/2}$)	K_{Ic} max (MPa m$^{1/2}$)	K_{Ic} min (MPa m$^{1/2}$)	S.d. (MPa m$^{1/2}$)
AS	9.1–**11.0**–13.0	17.0	6.1	3.6
T300	15.4–**20.3**–25.2	28.4	11.7	7.1
T400	13.4–**16.1**–18.9	22.4	11.1	4.5
Quenched	17.9–**19.7**–21.4	23.2	16.6	2.5

The average value of K_{Ic} is given (in boldface) with a 90% confidence interval according to student's criterion.

Table 2
Summary of results for the apparent dynamic fracture toughness K_{Id}

Group	K_{Id} average + 90% CI (MPa m$^{1/2}$)	K_{Id} max (MPa m$^{1/2}$)	K_{Id} min (MPa m$^{1/2}$)	S.d. (MPa m$^{1/2}$)
AS	47.2–**51.9**–56.6	74.0	27.3	13.4
T300	61.1–**68.0**–74.9	113.8	36.0	23.9
T400	57.2–**64.5**–71.4	121.8	17.3	26.3
Quenched	49.2–**58.9**–68.7	108.3	21.8	23.8

The average value of K_{Id} is given (in boldface) with a 90% confidence interval according to Student's criterion.

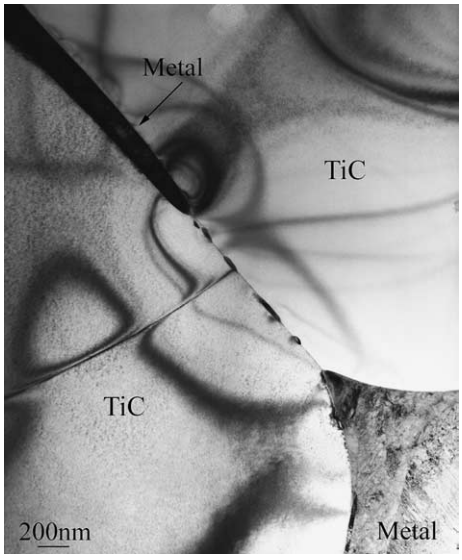

Fig. 1. Bright field TEM micrograph demonstrating penetration of the liquid metal, even into geometrically complex regions, indicating the good wetting in this system.

Small flaws were found at the metal-ceramic interfaces in the infiltrated and heat treated specimens (see Fig. 2). These flaws seemingly formed while the metal was solid, since otherwise their shape would be closer to a semi-spherical cap, as dictated by the contact angle [5,6]. It should be noted that in ceramic-matrix composites infiltrated with more ductile metals, such as Al or Cu [7,8], such interfacial flaws were not detected.

3.3. Microstructure after loading

While interfacial flaws were found in TEM specimens, regardless from where the specimens were cut from the bulk, cracking was found in TEM specimens sectioned parallel to the fracture surface of loaded samples. Significant differences could be found in the microstructure of the samples prior to and after mechanical loading, and as a function of the thermal treatment and static versus dynamic loading.

Static loading of the tempered samples resulted in mixed crack propagation along the TiC–TiC interface and inside the steel matrix. For example, the TEM micrograph of a sample statically loaded after tempering at 300 °C (Fig. 3) shows mixed interface and metal failure, in addition to the deformation of the previously flat interfacial flaws. Fig. 4 presents a TEM micrograph of a sample statically loaded after tempering at 400 °C. The micrograph was taken from a relatively thick region of the specimen, to demonstrate that sample thinning is

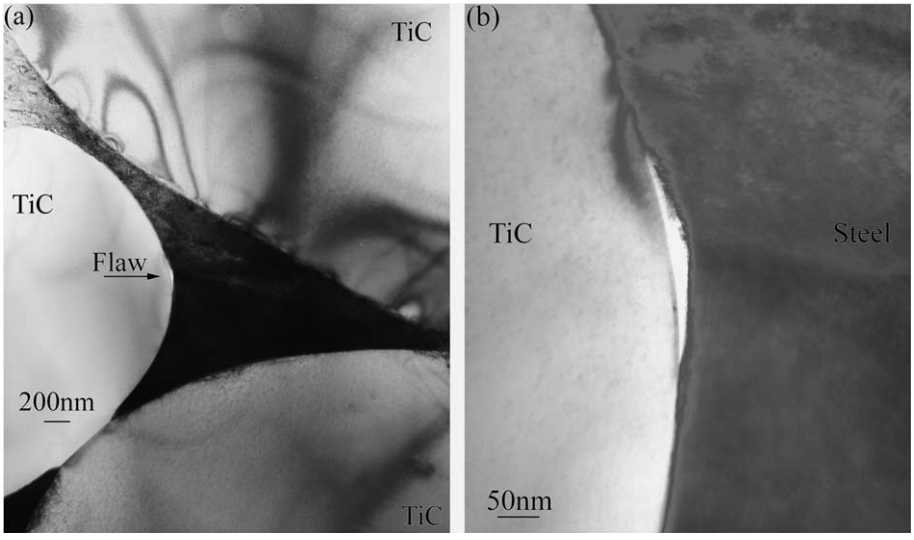

Fig. 2. Bright field TEM micrograph (a) of an interfacial flaw, in a specimen heat treated at 200 °C for 1 h after infiltration and austenization. A micrograph of the flaw at higher magnification is presented in (b), showing that the flaw is located at the metal–ceramic interface.

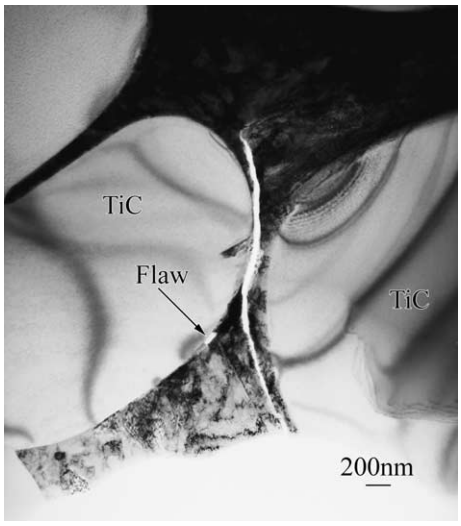

Fig. 3. Bright field TEM micrograph of a statically loaded sample, after tempering at 300 °C. Failure is by a mixed interface–metal mode of crack propagation. Previously flat interfacial flaws are rounded due to the static loading, indicating the ductile nature of the tempered metal.

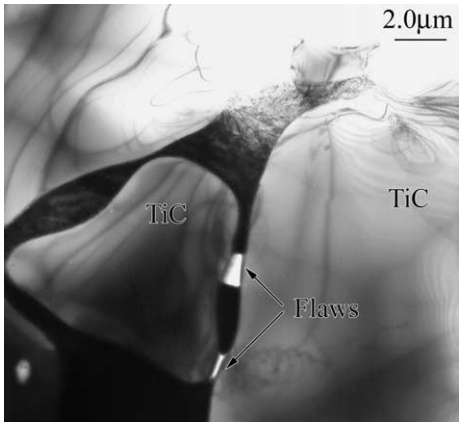

Fig. 4. Bright field TEM micrograph of a statically loaded sample, after tempering at 400 °C. Note the rounded (blunted) interfacial flaws.

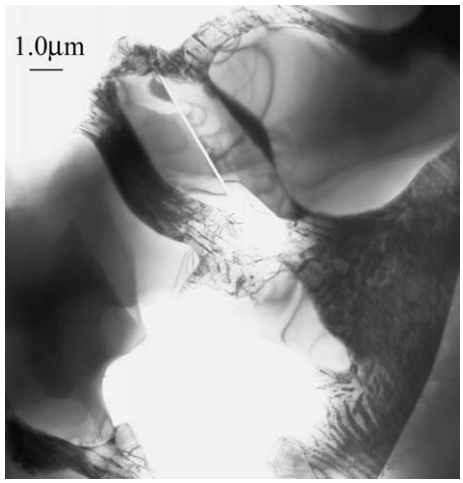

Fig. 5. Bright field TEM micrograph of an as-infiltrated sample, prepared from a fracture surface after dynamic testing.

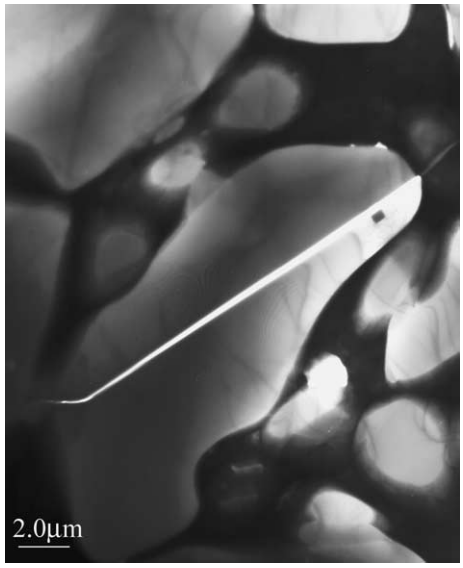

Fig. 6. Bright field TEM micrograph of a tempered sample (300 °C), prepared from a fracture surface after dynamic testing.

unrelated to the presence of deformed (blunted) interfacial flaws.

Dynamically loaded samples exhibited a significant amount of transgranular cracking of the TiC phase (see Figs. 5 and 6). While transgranular failure of the TiC was a dominant feature in the dynamically loaded specimens, grain boundary fracture of the TiC and some crack propagation through the relatively brittle metal was found in specimens after austenization, presumably a result of the more brittle nature of the martensitic phase (Fig. 7). Dynamic loading of more ductile specimens (after tempering) also resulted in rounded interfacial flaws (Fig. 8), and failure by interfacial fracture (Fig. 9), along with transgranular cracking of the TiC phase.

One may tentatively explain the observed toughening by two related effects. The first one is additional energy dissipation caused by the creation of numerous new surfaces (micro-cracks). The main crack front is thus surrounded by these micro-cracks, so that its formation and extension as a single crack front is delayed. At the characteristic stress intensity rate of $\dot{K} \approx 10^6$ $\mathrm{MPa}\sqrt{\mathrm{m}}\mathrm{s}^{-1}$, a delay of 5 μs in crack initiation is largely sufficient to cause the observed dramatic toughening.

4. Summary and conclusions

Mechanical damage mechanisms in TiC-1080 steel cermets have been characterized using TEM. The goal

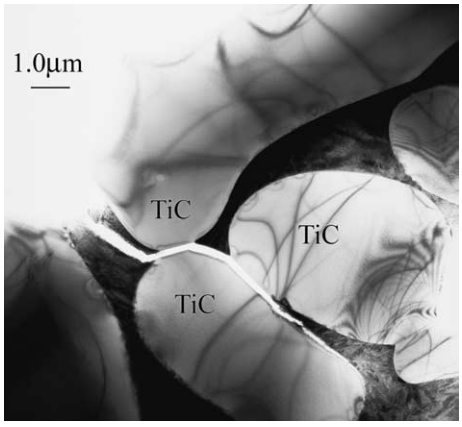

Fig. 7. Bright field TEM micrograph from a sample dynamically loaded after quenching from the austenization temperature. Fracture along the TiC grain boundaries and through the relatively brittle metal is visible.

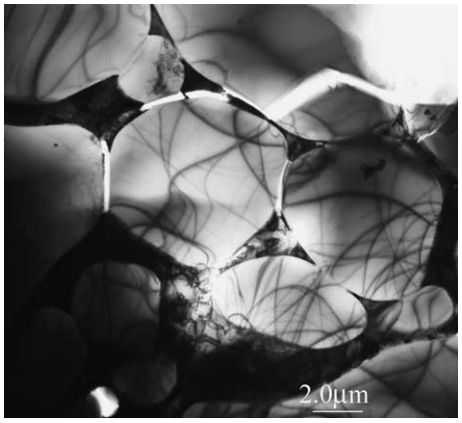

Fig. 9. Bright field TEM micrograph showing a mixed failure mode, including transgranular cracking, followed by interfacial fracture, in a sample dynamically loaded after tempering at 300 °C.

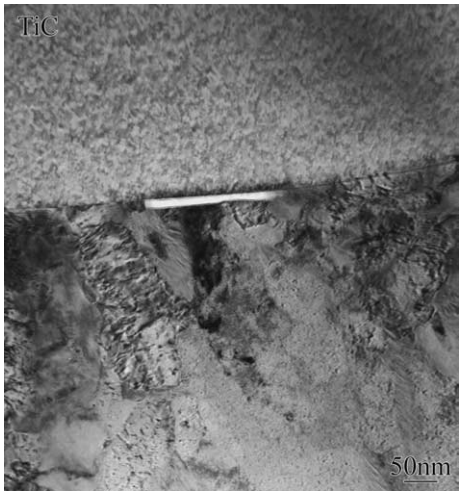

Fig. 8. Rounded interfacial flaws in the tempered (400 °C) and dynamically loaded specimens, indicating plastic deformation due to the relatively ductile metal.

of this study was to identify the failure micromechanisms that are responsible for the noticeable increase in the apparent dynamic initiation toughness of these materials, as compared to the quasi-static ones. While the present study is necessarily of a limited statistical character, it nevertheless shows distinct damage mechanisms. Firstly, and common to all the investigated samples, processing related damage appears in the form of interfacial flaws at the TiC-steel interface. These flaws are most likely related to the different thermal expansion coefficients of these materials. Quasi-static failure occurs by extension and blunting of these flaws, and also by grain boundary and interfacial cracking, with subsequent propagation into the steel matrix. By contrast, dynamic loading induces an additional failure mechanism that consists of transgranular TiC cracking without extension into the steel matrix. This additional specific failure mechanism can be related to the lower spall strength of the ceramic phase as compared to that of the steel matrix [1]. It is also deemed to consume additional energy, through the creation of numerous micro-cracks, their interaction among themselves and the main fracture surface. Dynamic transgranular cracking of the TiC phase is thus considered to contribute to the higher dynamic fracture properties of the investigated cermets by delaying crack initiation.

Acknowledgements

This research was partially supported by the Israeli Ministry of Science under grant No. 20562-01-99. Moshe Katz is acknowledged for his assistance with specimen preparation.

References

[1] Klein B, Frage N, Dariel MP, Zaretzky E. J Appl Phys 2003;93:968.
[2] Rittel D, Frage N, Dariel MP. Int J Solids Struct, 2004, in press.
[3] Weisbrod G, Rittel D. Int J Fracture 2000;104:89.
[4] Gonzalez EJ, Trumble KP. J Am Ceram Soc 1996;79:114.
[5] Dalgleish BJ, Saiz E, Tomsia AP, Cannon RM, Ritchie RO. Scripta Metall Mater 1994;31:1109.
[6] Bendixen J, Mortensen A. Scripta Metall Mater 1991;25:1917.
[7] Kaplan WD. Acta Mater 1998;46:2369.
[8] Scheu C, Dehm G, Kaplan WD. J Am Ceram Soc 2001;84:623.